THE JOURNAL OF BIOLOGICAL CHEMISTRY VOL. 287, NO. 37, pp. 30952–30966, September 7, 2012
© 2012 by The American Society for Biochemistry and Molecular Biology, Inc. Published in the U.S.A.

# Phosphorylation of Gephyrin in Hippocampal Neurons by Cyclin-dependent Kinase CDK5 at Ser-270 Is Dependent on Collybistin[S]

Received for publication, February 6, 2012, and in revised form, June 25, 2012 Published, JBC Papers in Press, July 9, 2012, DOI 10.1074/jbc.M112.349597

**Jochen Kuhse**[1], **Heba Kalbouneh, Andrea Schlicksupp, Susanne Mükusch, Ralph Nawrotzki, and Joachim Kirsch**
*From the Department of Anatomy and Cell Biology, University of Heidelberg, D-69120 Heidelberg, Germany*

**Background:** Formation of inhibitory synapses in the CNS is dependent on cluster formation of the scaffold protein gephyrin.
**Results:** Knockdown of collybistin and inhibition of cyclin-dependent kinases (CDK1,- 2, and -5) abolished the phosphorylation of gephyrin detected by mAb7a at Ser-270.
**Conclusion:** Gephyrin detected with mAb7a is phosphorylated at Ser-270.
**Significance:** These data suggest a novel view on kinases involved in gephyrin phosphorylation.

**Gephyrin is a scaffold protein essential for the postsynaptic clustering of inhibitory glycine and different subtypes of $GABA_A$ receptors. The cellular and molecular mechanisms involved in gephyrin-mediated receptor clustering are still not well understood. Here we provide evidence that the gephyrin-binding protein collybistin is involved in regulating the phosphorylation of gephyrin. We demonstrate that the widely used monoclonal antibody mAb7a is a phospho-specific antibody that allows the cellular and biochemical analysis of gephyrin phosphorylation at Ser-270. In addition, another neighbored epitope determinant was identified at position Thr-276. Analysis of the double mutant gephyrin$^{T276A,S277A}$ revealed significant reduction in gephyrin cluster formation and altered oligomerization behavior of gephyrin. Moreover, pharmacological inhibition of cyclin-dependent kinases in hippocampal neurons reduced postsynaptic gephyrin mAb7a immunoreactivities. *In vitro* phosphorylation assays and phosphopeptide competition experiments revealed a phosphorylation at Ser-270 depending on enzyme activities of cyclin-dependent kinases CDK1, -2, or -5. These data indicate that collybistin and cyclin-dependent kinases are involved in regulating the phosphorylation of gephyrin at postsynaptic membrane specializations.**

The formation of clusters of inhibitory glycine receptors (GlyR)[2] and some subtypes of $GABA_A$ receptors at the postsynaptic membrane strictly requires the scaffold protein gephyrin (1). It is believed that gephyrin-dependent cluster formation is achieved by anchoring receptors to the microtubular and actin-based cytoskeleton (2). However, the molecular mechanisms regulating the precise localization and size of gephyrin and GlyR/$GABA_A$ receptor clusters within the somatodendritic compartments are not completely understood. Collybistin (Cb), a gephyrin binding guanidine exchange factor for the monomeric GTPase Cdc42 (3, 4) may regulate local cluster formation by interaction with the cell adhesion protein neuroligin II (5). Studies of Cb knock-out mice revealed a reduction of gephyrin and γ2-containing $GABA_A$ receptor clusters in hippocampus and cerebellum, whereas GlyR clusters in spinal cord neurons were unaltered (6). Thus, the functional role(s) of Cb in different areas of the CNS remains to be established (7, 8).

In rat, four alternative spliced Cb isoforms have been described (Cb1–4). All variants possess a central tandem dbl-homology (DH)/pleckstrin homology (PH)-domain; apparently a functional PH-, but not DH-domain, is required for proper function (9). Moreover, one isoform (Cb2) exists with and without an src-homology-3 ($SH_3$)-domain near the N terminus (3, 4).

The domain structure of gephyrin is composed of an N-terminal G-domain and a C-terminal E-domain. Isolated G- and E-domains form trimers and dimers, respectively, and thus were proposed to cause the formation of a hexagonal lattice of gephyrin at the postsynaptic membrane (10). Both domains are connected by the central C-domain, which harbors binding sites for several gephyrin interacting proteins (11).

GlyRs and $GABA_A$ receptor are pentameric receptor complexes. The homologous subunits contain four transmembrane domains (TM1–4), and the extended cytoplasmic loop between the TM3 and TM4 regions (12, 13) of the GlyR β subunit mediates the binding to gephyrin (14, 15), whereas the homologous region of the GlyR α2 subunit may bind different kinases and calcineurin (16). Whereas the binding of gephyrin to the GlyR was evident from GlyR purification studies and was analyzed in great detail (10, 17, 18), it has only recently been shown that a similar site on gephyrin also binds directly to $GABA_A$ receptor subunits α1, α2, and α3 (19–21).

Phosphorylation of gephyrin was first reported in 1992 (22). More recently, the binding of gephyrin to the peptidyl-prolyl *cis*/*trans*-isomerase Pin1 was analyzed and allowed the identification of amino acid residues (Ser-188, Ser-194, and Ser-200) in the C-domain as major determinants of phosphorylation

[S] This article contains supplemental Figs. 1 and 2.
[1] To whom correspondence should be addressed: Universität Heidelberg, Institut für Anatomie und Zellbiologie, Lehrstuhl II, Im Neuenheimer Feld 307, D-69120 Heidelberg, Germany. Tel.: 49-6221-548663; Fax: 49-6221-544952; E-mail: jochen.kuhse@urz.uni-heidelberg.de.
[2] The abbreviations used are: GlyR, glycine receptor; Cb, Collybistin; PH, pleckstrin homology; CDK, cyclin-dependent kinase; VIAAT, vesicular inhibitory amino acid transporter; GSK, glycogen synthase kinase.

dependent Pin1 binding and also of gephyrin clustering (23). In addition, Ser-270 was identified as another phosphorylation site that was reported to be phosphorylated by GSK3$\beta$ (24). Exchange of Ser-270 by alanine in that study increased gephyrin cluster numbers, suggesting an inhibitory role of phosphorylation at this site. Moreover, another study demonstrated that the inhibition of phosphatase 1 decreased gephyrin cluster size in cultured hippocampal neurons (25).

The precise role of Cb and Cdc42 in receptor clustering is still not well understood. One current model of Cb function proposes that the N-terminal SH3 domain present in the Cb splice variants Cb1, $Cb2_{+SH3}$, and Cb3 inactivates Cb. The binding to SH3-domain-interacting proteins, like neuroligin II or the cytoplasmic loop of the $GABA_A$ receptor $\alpha$2 subunit, may activate Cb, which consequently would mediate local specific gephyrin clustering by an unknown molecular mechanism (5, 19). A conditional Cdc42 knock-out mouse revealed no alteration of gephyrin cluster formation (9). More recently, however, cotransfection experiments with Cb mutants and constitutively active Cdc42 suggested an important contribution of Cdc42 to gephyrin clustering, possibly by forming a ternary complex with gephyrin and $Cb2_{-SH3}$ (26).

To study the functional role of Cb, we performed Cb-shRNA knockdown experiments in cultured hippocampal neurons. Interestingly, a decrease of Cb expression resulted in a reduction of gephyrin phosphorylation. Pharmacological inhibition of specific kinase pathways showed that cyclin-dependent kinases (CDKs) are involved in phosphorylation of gephyrin at Ser-270. Thus, our results are consistent with a model of cluster formation at inhibitory postsynaptic membrane specializations in which Cb increases gephyrin phosphorylation at Ser-270, a process that can be monitored by the phosphospecific antibody mAb7a (27).

## EXPERIMENTAL PROCEDURES

*Construction of Expression Plasmids and Knockdown Vectors*—DNA fragments encoding the complete coding sequence of rat gephyrin (P1 clone) (28) were amplified by PCR, creating SfrI flanking restriction sites, and were cloned in the expression vector pCMVTAG3B (Invitrogen), resulting in N-terminal fusion constructs with a myc epitope (myc-gephyrin). N-terminally 6×-histidine-tagged gephyrin-coding PCR products with flanking NotI and XhoI sites were cloned into vector pcDNA5/FRT/TO (Invitrogen). All constructs were verified by sequence analysis. Sequences coding for a shRNA directed toward Cb and control shRNA were cloned into pFSGW, a modified version of the lentiviral vector pFUGW (29) using the human synapsin promoter to drive EGFP expression as described in Körber *et al.* (30) (CB-shRNA-coding sequence 5′-TTTGAATCCGGAGAGACATCCTATAGTGAAGCCACAGATGTATAGGATGTCTCTCCGGATTTTTTT-3′ or an unrelated control sequence, 5′-TTTGTTGGTCTTGTGGCATTACAGTGAAGCCACAGATGTGTAATGCCACAAGACCAATTTTT-3′.

*Site-directed Mutagenesis*—Site-directed mutagenesis of gephyrin-P1 clone, $His_6$-gephyrin, or myc-gephyrin was performed using the QuikChange Lightning mutagenesis kit from Stratagene following the supplier's instructions. Mutants were verified by sequence analysis.

*Lentivirus Preparation*—Recombinant lentiviral particles were produced as described in Körber *et al.* (30).

*Cell Culture*—Primary cultures of rat hippocampal neurons were prepared from E19 embryos plated at a density of 60.000 cells/$cm^2$ and transfected as described previously (31). Infection with lentivirus dilutions and transfection of cells with expression plasmids was performed 2 days after plating (div2). Fixation and immunocytochemistry was done either at div9, div14, or div21.

*Immunocytochemistry*—Immunocytochemistry was performed as described in Körber *et al.* (30) with the following modifications. Cultured neurons were washed once with PBS at 37 °C and fixed with cold methanol (−20 °C) for Ab-175 stainings for 10 min. Cells were incubated with the primary antibody dilutions as described in Körber *et al.* (30) and with the following modifications: mouse monoclonal anti-gephyrin mAb7a (27) (1:200), mouse monoclonal anti-gephyrin mAb5 (27) (1:500); rabbit anti-gephyrin Ab-175 (32) (1:250), and anti-Cb antibody (1:10, BD Transduction, catalog no. 612076. For colocalization studies and quantifications, MetaMorph software was used. To evaluate the amount of colocalization with each receptor type or synaptic marker, three dendritic regions with a length of 30 $\mu$m were chosen. After setting the same threshold for these regions in one experiment, the quantification of the colocalization of gephyrin with the VIAAT immunoreactivity was determined by the software and by visual inspection. Data analysis was done using Excel and Prism software.

*Transfection of HEK293T Cells for Cb- and Gephyrin Coexpression Experiments*—HEK293T cells cultured in 6-well plates were transfected with expression constructs using polyethyleneimine (PEI) (Sigma). A total of 6 $\mu$g of plasmid DNA (3 $\mu$g of myc-gephyrin + 3 $\mu$g of empty vector or 3 $\mu$g of $Cb2_{-SH3}$ expression plasmid (3)) was incubated in Opti-MEM® (Invitrogen) medium in the presence of PEI for 30 min (77 $\mu$g/ml) before adding it to 2 ml of DMEM (Invitrogen) + 10% (v/v) FCS (PAN) medium of the HEK293T cell culture and incubated for 4 h in a humidified incubator at 37 °C and 5% $CO_2$. After exchanging the medium with DMEM medium supplemented with 10% (v/v) FCS and 1% (v/v) PenStrep (penicillin/streptomycin) (Invitrogen), cells were incubated for another 24 h under the same conditions before they were harvested.

*Pharmacological Treatment of HEK293T Cells and Preparation of Protein Extracts*—HEK293T cells were cultured in 6-well plates, transfected with expression constructs of myc-tagged gephyrin and $Cb2_{-SH3}$ (3), treated with the indicated concentrations of kinase inhibitors overnight, and homogenized after about 24 h in ice-cold lysis buffer: 50 mM Tris-HCl, pH 7.5, 150 mM NaCl, 1% (v/v) nonylphenoxylpolyethoxylethanol (Nonidet P-40), 0.25% (w/v) sodium dodecyl sulfate (SDS), 2 mM sodium orthovanadate, and protease inhibitor mixture (complete, Roche Applied Science). Chromosomal DNA was shortened by passing the extract through a cannula. After centrifugation for 30 min at 4 °C at 16 000 × *g*, supernatants were used for immunoblot analysis.

*Pharmacological Treatment of Cultured Neurons*—Hippocampal neurons were cultured for 9 days *in vitro* in 24-well

plates. At div2, div5, and div6, cell culture medium was supplemented with small volumes of appropriate stock solutions (0.05% (v/v)) of the inhibitors solubilized in DMSO. In other experiments hippocampal neurons were cultured for 14 days, and inhibitor was added 1, 3, 6, or 24 h before fixation. Identical volumes of DMSO were used as controls. After incubation at 37 °C at 5% $CO_2$ in a humidified cell culture incubator, cells were fixed and stained as described above.

*Immunoblot Analysis*—Western blotting as described in Körber *et al.* (30). Membranes were probed with mouse monoclonal mAb7a antibody (1:200), rabbit anti-gephyrin antibody Ab-175 (1:200) (32), and anti-myc antibody (1:200, Santa Cruz, catalog no. Sc-789), and anti-Cb antibody (1:100, BD Transduction Laboratories catalog no. 612076). After suitable exposure times, films were developed, and signals were scanned and analyzed using Kodak Digital science 1D or Fiji software.

*Peptide Competition Assay*—Immunoblots were done with protein extracts from HEK293T cells coexpressing gephyrin and $Cb2_{-SH3}$. mAb7a antibody was preincubated with peptides with concentrations from 2 to 0.25 mg/ml in 50 $\mu$l of TBS-Tween (30) with a 1:20 dilution of mAb7a for 1 h at room temperature. After a centrifugation step (13,200 rpm, 15 min), the preincubated mAb7a/peptide solution was further diluted 10-fold with blocking solution (30) and applied to immunoblots using PVDF membrane stripes. The further procedure was as described above for immunoblots. Experiments were done 3–6-fold (P270) times.

*Phosphatase Treatment of Neuronal Protein Extracts*—Neurons plated on 6-well plates were scraped at div23 in lysis buffer without sodium orthovanadate and homogenized as described above. λ-Phosphatase (Sigma, P9614) treatment was done in a volume of 60 $\mu$l at 30 °C for 30 min. 400 units of λ-phosphatase were used in 50 mM Tris-HCl, pH 7.5, 0.1 mM $Na_2EDTA$, 5 mM dithiothreitol, 0.01% BRIJ 35, and 2 mM $MnCl_2$ with about 40 $\mu$g total neuronal protein extract. Reactions were stopped with gel-loading buffer, and samples were heated to 95 °C for 5 min.

*Protein Extracts for Cb Knockdown Analysis*—Neurons were plated with $4 \times 10^5$ cells/well in a 6-well plate and infected at div2 with an 8-fold higher number of virus particles than in 24-well plate cultures, which were used to monitor infection rate. Cells were scraped at div23 and homogenized in lysis buffer as described above.

*Gephyrin Purification*—HEK293T cells (grown on 20 × 10-cm plates with 10-ml volumes of DMEM (Invitrogen) + 10% (v/v) FCS (PAN)) were transfected with $His_6$-tagged gephyrin expression vector. 15 $\mu$g of plasmid DNA/plate was used for transfection as described above. After 2 days of incubation in a humidified incubator at 37 °C and 5% $CO_2$, cells were homogenized with a Dounce Homogenizer Potter-Elvehjem on ice in 10 mM phosphate buffer, pH 7.3, 137 mM NaCl, 3 mM KCl, 2 mM sodium orthovanadate ($Na_3VO_4$) and protease inhibitor mixture (Roche Applied Science, complete). $His_6$-tagged gephyrin was purified under native conditions on an Ettan LC purification unit from cleared cell supernatant (centrifugation at 4 °C, 20 000 × *g*, 30 min) with nickel-nitrilotriacetic acid-Sepharose (Ni-Sepharose™ 6 Fast Flow, GE Healthcare, no. 17-5318-06) using 100 mM imidazole in phosphate buffer (see above) for column washing and 500 mM imidazole in phosphate buffer for elution of recombinant gephyrin.

*In Vitro Phosphorylation Assay*—Identical amounts of purified $His_6$-gephyrin were used for *in vitro* phosphorylation assays performed in HEPES buffer (60 mM, pH 7.6 with 1 mM ATP, 12.5 mM $MgCl_2$, 1 mM DTT, and 0.1–0.4 units of CDK1/cyclinB, CDK2/cyclinA, or CDK5/p35NCT protein complexes (Biaffin, Kassel, Germany) at 30 °C for 30 min. The reaction was stopped with SDS-PAGE loading buffer, and proteins were analyzed by immunoblotting as described above.

*In Vitro $^{32}P$ Phosphorylation Assay*—For immunoprecipitation of $^{32}P$-labeled gephyrin, the gephyrin-specific antibody mAb5 (27) was prebound to protein A/G-agarose (Pierce, Thermoscientific) by adding 40 $\mu$l of protein A/G-agarose and 50 $\mu$l of mAb5 solution in 150 $\mu$l of 20 mM Tris/HCl, pH 7.5, 200 mM NaCl, 1 mM EDTA, 10% (v/v) glycerol, and 0.1% (v/v) Nonidet P-40 (immunoprecipitation buffer) and incubated at 4 °C for 1 h, and bound mAb5 was sedimented with protein A/G-agarose by centrifugation for 5 min at 4 °C at 13,200 rpm and 2× washed with immunoprecipitation buffer. Identical amounts of purified $His_6$-gephyrin were used for *in vitro* phosphorylation assays performed as described above with 50 $\mu$Ci of [$\gamma$-$^{32}$P]ATP replacing ATP. The reaction was stopped with 10 $\mu$l of EDTA (0.2 M) and added to 170 $\mu$l of resuspended protein A/G-agarose with prebound mAb5. After incubation at 4 °C for 1 h, gephyrin bound to mAb5-protein A/G-agarose was sedimented by centrifugation for 5 min at 14,500 rpm at 4 °C, and the pellet was washed 3 times with 500 $\mu$l of ice-cold immunoprecipitation buffer. Gephyrin was solubilized from mAb5-protein A/G-agarose with 20 $\mu$l of 4× SDS-PAGE loading buffer at 95 °C for 5 min, and proteins were separated on 4–12% polyacrylamide gradient SDS-gels (NuPAGE Novex Bis-Tris mini gels, Invitrogen). Gels were stained to control for equal loading with Coomassie Blue and dried on a vacuum gel dryer and exposed to x-ray Kodak films.

*Co-immunoprecipitation*—For immunoprecipitation, 1 mg of protein lysate (see above, lysis buffer: 20 mM Tris-HCl, pH 7.4, 150 mM NaCl, 1 mM EDTA,10% glycerol, 1% Nonidet P-40, 0.1% SDS, 2 mM sodium orthovanadate, and protease inhibitor mixture (complete, Roche Applied Science)) was incubated with 2 $\mu$g of rabbit polyclonal anti-CDK5 antibody (C-8, Santa Cruz, catalog no. Sc173) or rabbit anti-VGAT antibody (Synaptic Systems, catalog no. 131011) as control at 4 °C overnight with rotation. 25 $\mu$l of protein A/G-agarose prewashed with lysis buffer was added and rotated at 4 °C for 4 h. After 4× washing with immunoprecipitation washing buffer (50 mM Tris/HCl, pH. 8.0, 150 mM NaCl, 1% Nonidet P-40), the immunoprecipitated proteins were solubilized in 10 $\mu$l of 4× SDS-PAGE loading buffer at 95 °C for 5 min (with 8 M urea) and analyzed by immunoblotting.

*Statistical Analysis*—Experimental data were evaluated without knowledge of the experimental conditions used for at least three independent experiments. Statistical analysis was performed using the GraphPad-prism IV software with non-parametric analysis of variance followed by Tukey's multiple comparison test; other data were analyzed with Student's *t* test. Data are shown the means ± S.E. or S.D. Values of $p < 0.05$ were considered as significant.

*Ethical Treatment of Animals*—This study was carried out in strict accordance with the European Communities Council Directive (86/609/EEC) to minimize animal pain or discomfort. The animal care and use committee gave approval for the study under number T-81/10.

## RESULTS

*Cb Knockdown Abolishes the Formation of Gephyrin Clusters in Hippocampal Neurons*—To elucidate the functional role of Cb in GlyR and $GABA_A$ receptor clustering, we performed Cb knockdown experiments with cultured rat hippocampal neurons. Neurons were infected with Cb-shRNA lentivirus (Cb-shRNA), a control-shRNA lentivirus, or a combined Cb-knockdown-$Cb2_{-SH3}$ rescue lentivirus 1 day after plating. After 2–3 weeks *in vitro* differentiation (div14/div21), formation of gephyrin clusters was monitored by immunofluorescence microscopy. Interestingly, we observed a nearly complete loss of mAb7a gephyrin puncta in most Cb-shRNA-infected cells, whereas the staining of presynaptic vesicular inhibitory amino acid transporter (VIAAT) was still preserved (Fig. 1*A*″), an observation that is in agreement with the results of gephyrin staining in hippocampal preparations from Cb knock-out mice (6). Importantly, $Cb2_{-SH3}$ rescue virus-infected cells with shRNA-mediated knockdown of endogenous Cb and simultaneously expressing $Cb2_{-SH3}$, which is shRNA-insensitive, showed gephyrin clusters stained with mAb7a very similar to control cells (Fig. 1*A*‴), indicating that the loss of mAb7a puncta in the Cb-knockdown experiment was due to the specifc knock-down of Cb. Control staining with an antibody specific for Cb revealed a strong reduction of Cb-staining in Cb-shRNA expressing cells (Fig. 1*B*). Examination of excitatory synapses by staining with anti-PSD95 antibody showed no significant alteration (data not shown). Thus, reduction of Cb expression in hippocampal neurons reduced the staining of gephyrin clusters with mAb7a specifically (for a more detailed functional analysis of Cb knockdown experiments, see Ref. 30).

*Cb Knockdown Results in Alteration of the mAb7a Epitope on Gephyrin*—The strong reduction of mAb7a immunoreactivity suggested a down-regulation of gephyrin expression as a consequence of Cb knockdown. To get further support for this conclusion, we performed immunoblot analyses with protein extracts of cultured hippocampal neurons infected with Cb-shRNA or control viruses. As already seen with immunofluorescence experiments (Fig. 1, *A*″ and *B*), there was a robust reduction of Cb and mAb7a immunoreactivities upon Cb knockdown (Fig. 1*C*). In protein extracts from control virus-infected cells or non-infected cells, mAb7a detected two closely migrating bands with an apparent molecular mass of around 93 kDa (Fig. 1*C*′). Surprisingly, the use of another gephyrin-specific antibody (Ab-175) raised against a peptide of the C-domain (32) revealed a clear detection of both gephyrin bands also in extracts from Cb knockdown cells (Fig. 1*C*). This observation can be explained if one assumes that 1) the gephyrin epitope recognized by mAb7a is sensitive to posttranslational modifications, and 2) that the alterations of the mAb7a epitope on gephyrin depend on collybistin expression.

Earlier studies reported that gephyrin in GlyR preparations from rat spinal cord is phosphorylated (22). Therefore, we used phosphatase treatment to remove all phosphates from gephyrin and compared the binding of mAb7a and Ab-175 antibodies in immunoblots. As shown in Fig. 1*C*, removal of phosphate groups by phosphatase resulted in the complete loss of mAb7a immunoreactivity (Fig. 1*C*″). In contrast, gephyrin was clearly detected by Ab-175 anti-gephyrin antibody. However, there was a shift of one or both gephyrin bands toward lower molecular masses, indicating that gephyrin might be phosphorylated at a number of sites.

To further determine whether phosphorylation of gephyrin was indeed altered in Cb knockdown experiments, we set out to identify putative phosphorylation sites of gephyrin using site-directed mutagenesis. Heterologous expression in HEK293T cells was chosen as experimental system. The analysis of protein extracts from gephyrin-expressing cells showed that there was a similar loss of mAb7a immunoreactivity after phosphatase treatment (data not shown), suggesting that similar post-translational modifications at the phosphorylation-sensitive mAb7a epitope occur in HEK293T cells, although the level of immunoreactivity with mAb7a in general was lower than that observed for hippocampal neurons. Moreover, only one single band was detected upon heterologous expression of gephyrin in HEK293T cells.

Gephyrin contains more than 100 serine and threonine residues from which a large number might be regarded as putative phosphorylation sites. To narrow down candidate regions for site-directed mutagenesis analysis, we expressed different subdomains of gephyrin in an expression vector equipped with an N-terminal myc epitope tag in HEK293T cells. Immunoblot analysis of cell extracts showed that a protein consisting of the C-domain and the E-domain or the C-domain and the G-domain was detected by mAb7a. In contrast, the G-domain and E-domain without fused C-domain were not detected by mAb7a, indicating that the phosphorylation-sensitive epitope of mAb7a may be localized within the C-domain (data not shown).

The C-domain comprises about 170 amino acid residues with around 40 serine or threonine residues. Residues predicted to be localized at the protein surface were first chosen to be mutagenized to alanine in a non-tagged full-length gephyrin (P1) (28). Mutations were often performed in pairs with neighbored serine or threonine residues. Out of a set of mutants analyzed first, two gephyrin mutants ($gephyrin^{S268A,S270A}$ and $gephyrin^{T276A,S277A}$) revealed a strong reduction of mAb7a immunoreactivity, whereas immunosignals of Ab-175 were not reduced (Fig. 2). These results support the idea that mAb7a is a phospho-specific antibody and that the detection of the mAb7a epitope depends on phosphorylation within both of these two regions (Ser-268/Ser-270 and Thr-276/Ser-277). Moreover, this finding is in agreement with the report that Ser-270 is phosphorylated by GSK3$\beta$ (24).

*Mutations in the Gephyrin Central Domain Alter Gephyrin Cluster Formation and Polymerization in Cultured Hippocampal Neurons*—To further test the hypothesis that the loss of mAb7a epitope and reduced cluster numbers after Cb knockdown were functionally related to reduced phosphorylation in the region comprising determinants of the mAb7a epitope, we expressed myc-tagged wild-type gephyrin (myc-gephyrin)

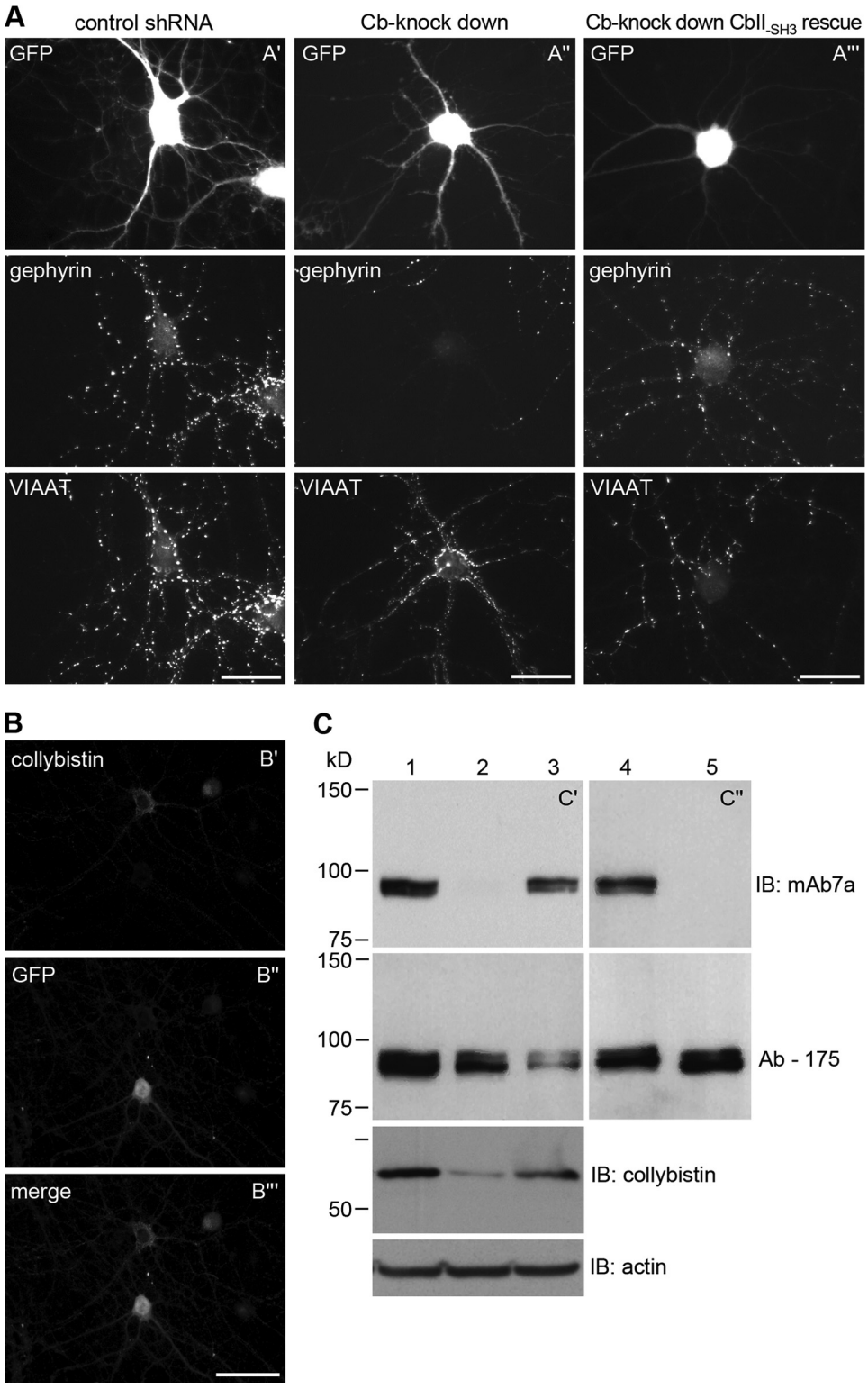


FIGURE 1. **Collybistin knockdown and phosphatase treatment results in the loss of mAb7a epitopes on gephyrin.** *A*, shown is immunofluorescence analysis of collybistin knockdown experiments. mAb7a (gephyrin) and VIAAT staining of div14 stages of hippocampal neurons that were infected, indicated by GFP staining, with control virus (*A'*), with collybistin shRNA lentivirus (A''), and with Cb2$_{-SH3}$ rescue virus (A'''). Note the strong reduction of mAb7a staining in A''. *Scale bar* is 30 $\mu$m. *B*, shown is immunohistochemical staining of collybistin in a collybistin shRNA-infected hippocampal culture as indicated by GFP staining. Note the collybistin expression in a non-infected cell, whereas the infected cell reveals no collybistin staining. *C*, cell lysates from cultured hippocampal neurons from control cultures (*lane 1*) or cultures infected with collybistin shRNA lentivirus (*lane 2*) or infected with control virus (*lane 3*) and protein extracts from hippocampal cultures, mock-treated (*lane 4*) or treated with λ-phosphatase (*lane 5*) were analyzed by SDS-PAGE and immunoblot (*IB*) experiments using mAb7a (*upper panel*, *C'*, *C''*) and Ab-175 (*lower panel*). *Below*, staining of another membrane with a collybistin-specific antibody demonstrated the reduction of collybistin in collybistin shRNA lentivirus-infected neuron cultures. Anti-actin staining was used as a loading control.

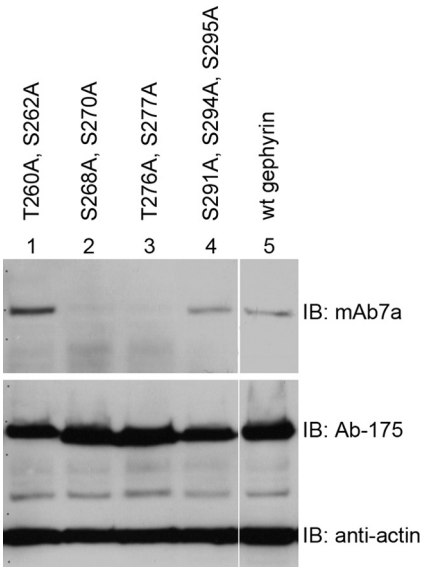


FIGURE 2. **Mutations at putative phosphorylation sites within the gephyrin linker region reduce binding of mAb7a.** Recombinant gephyrin (P1) was expressed in HEK293T cells, and protein extracts were analyzed by immunoblotting (*IB*). Wild-type gephyrin (*lane 5*) was detected with mAb7a and with an antibody directed against the gephyrin linker region (Ab-175). Mutations of two serines (Ser-268, Ser-270) (*lane 2*) or of a pair of threonine and serine (Thr-276, Ser-277) (*lane 3*) to alanine residues reduced the binding of mAb7a to the expressed protein, whereas mutations at positions 260, 262, 291, 294, and 295 did not reduce mAb7a signal intensities.

and myc-tagged gephyrin mutants (gephyrin$^{S268A,S270A}$ and gephyrin$^{T276A,S277A}$) in cultured hippocampal neurons stained for gephyrin with mAb7a and anti-myc antibody and for the γ2-subunit of $GABA_A$ receptors, and protein expression was analyzed with fluorescence microscopy. Our data analysis revealed that myc-gephyrin formed clusters that were apposed to $GABA_A$ receptor clusters at the cell soma and along branched dendrites indistinguishable compared with mAb7a puncta (Fig. 3*A′*). Also the double mutant (gephyrin$^{S268A,S270A}$) formed clusters and colocalized with γ2-containing $GABA_A$ receptors, suggesting that postsynaptic $GABA_A$-receptors were formed (Fig. 3*A″*). However, the cellular localization of mutant gephyrin$^{T276A,S277A}$ was different; 1) a lower number of gephyrin clusters was observed (Fig. 3*C*), and 2) in contrast to myc-gephyrin, this mutant formed elongated protein structures in the soma and in the dendritic tree (Fig. 3*A‴*). These elongated structures resembled those that were reported recently to result from transfection of hippocampal neurons with Cb mutated in the PH-domain (26). Moreover, a gephyrin mutant with alanine replacements at all four positions (gephyrin$^{S268A,S270A,T276A,S277A}$) also revealed long needle-like structures upon expression in hippocampal neurons (Fig. 3*B*).

Colocalization of recombinant gephyrin with clustered endogenous gephyrin could be concluded from expressing gephyrin$^{S268A,S270A}$ followed by the double staining with mAb7a and myc antibodies, as the mutant is not recognized by mAb7a. Interestingly, mAb7a staining of endogenous clustered gephyrin was significantly reduced when expressing mutants gephyrin$^{T276A,S277A}$, indicating a dominant negative effect of this mutant on endogenous gephyrin (Fig. 3*A‴*). The needle-like structures may be formed within the cell soma and within the neurite compartments because these mutations may affect the multimerization of gephyrin, and the needle-like protein structures may have trapped endogenous gephyrin.

To demonstrate that the loss of mAb7a immunoreactivity in Cb knockdown experiments was indeed due to the reduction of gephyrin at postsynaptic sites, we combined the expression of myc-gephyrin in hippocampal neurons with Cb knockdown virus infections. Interestingly, upon Cb knockdown in myc-gephyrin-transfected cells, recombinant myc-gephyrin did not form regular gephyrin clusters but was localized diffusely and in a few larger aggregates in dendrites and large protein aggregates in the cell soma (data not shown). In addition, we performed staining experiments with the anti-gephyrin antibody mAb5 (28) at div14 stages of Cb-shRNA-infected hippocampal neurons and confirmed a loss of gephyrin clusters (data not shown). Thus, these experiments also showed that indeed gephyrin clustering and not only gephyrin phosphorylation is reduced upon Cb knock-down.

*The Phosphorylation of Gephyrin in HEK293T Cells Is Dependent on GSK3β and CDKs*—Next, we analyzed the putative involvement of different kinases in the phosphorylation of gephyrin as monitored by mAb7a staining upon gephyrin expression in HEK293T cells. Interestingly, several phosphorylation sites within the central domain of gephyrin were identified by mass spectrometry upon screening for protein phosphorylation during the cell cycle in a human cell line (33). These data indicated that cell cycle-specific kinases like CDKs might be involved in phosphorylation of gephyrin. Indeed several sites within the linker region of gephyrin are predicted to be phosphorylated by either CDK1 (CDC2) or CDK5 (NetPhosK 1.0 Server); therefore, we set out to investigate the contribution of different kinases to gephyrin phosphorylation using inhibitors for CDKs and GSK3β, which was published to phosphorylate gephyrin at Ser-270 (24). First, we compared single expression of gephyrin to coexpression of gephyrin and $Cb2_{-SH3}$. Interestingly, coexpression of $Cb2_{-SH3}$ with gephyrin strongly increased the signal intensities observed on mAb7a immunoblots of protein extracts from transfected cells (Fig. 4). Moreover, coexpression of $Cb2_{-SH3}$ resulted in the appearance of a second gephyrin band with a higher apparent molecular mass (Fig. 4*A*). This observation might be relevant to understand the presence of two gephyrin bands also in protein extracts from neurons (see Fig. 1*C*). Interestingly, the presence of either 10 μM GSK3β inhibitor AR-A014418 or 5 μM CDK inhibitor aminopurvalanol A abolished the increase of mAb7a signal intensities in extracts containing recombinant gephyrin coexpressed with $Cb2_{-SH3}$ and also significantly decreased the low intensities of mAb7a immunoreactivity seen with gephyrin expression alone (Fig. 4, *A*, *B*, and *B′*).

These results demonstrate that protein kinases affect gephyrin in a way that mAb7a binding to gephyrin is increased. Moreover, these data provide evidence that phosphorylation of gephyrin is dependent on the presence of Cb, CDK, and GSK3β enzymatic activities and can be monitored by mAb7a binding.

*Characterization of the Phosphorylation-dependent mAb7a Epitope within the C-domain of Gephyrin*—To further corroborate that the alteration of mAb7a epitope recognition of gephyrin upon coexpression with $Cb2_{-SH3}$ is dependent on phosphorylation, we set out to further characterize the mAb7a

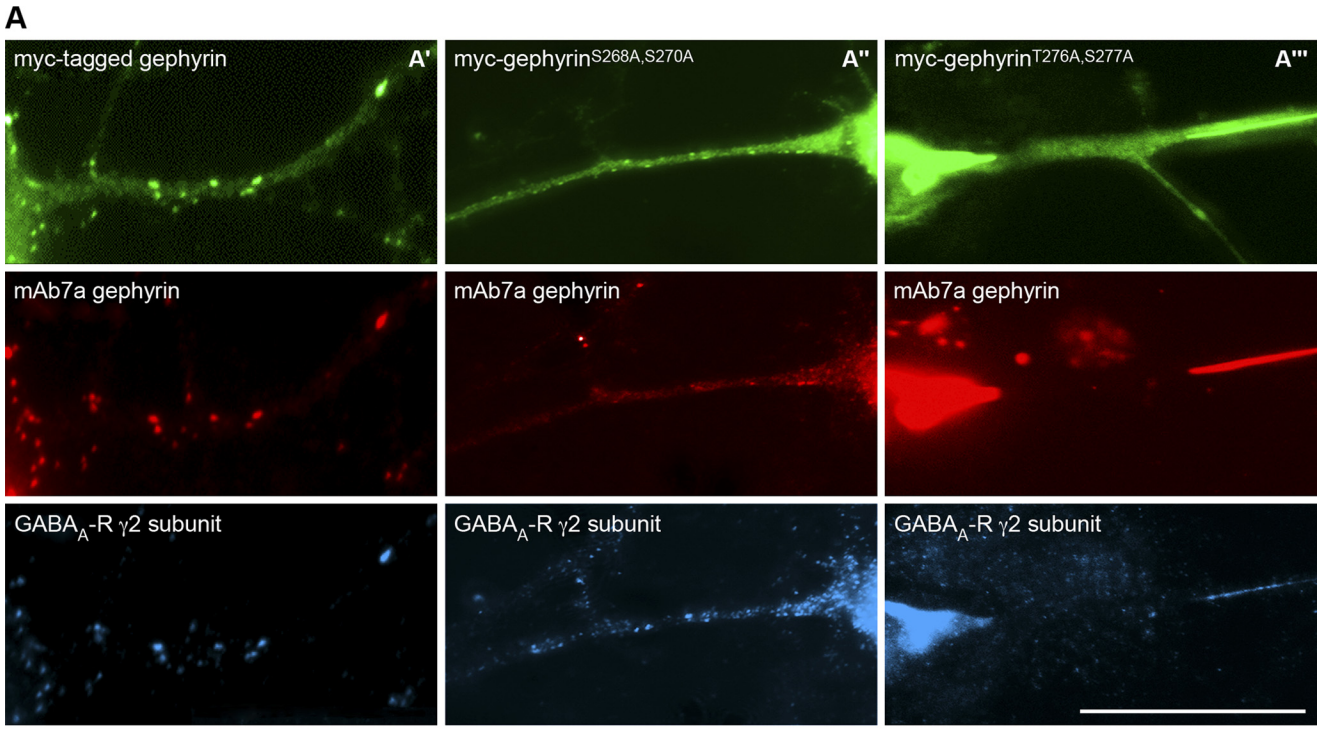
A
myc-tagged gephyrin
A'
myc-gephyrin S268A,S270A
A''
myc-gephyrin T276A,S277A
A'''
mAb7a gephyrin
mAb7a gephyrin
mAb7a gephyrin
GABA A -R γ2 subunit
GABA A -R γ2 subunit
GABA A -R γ2 subunit

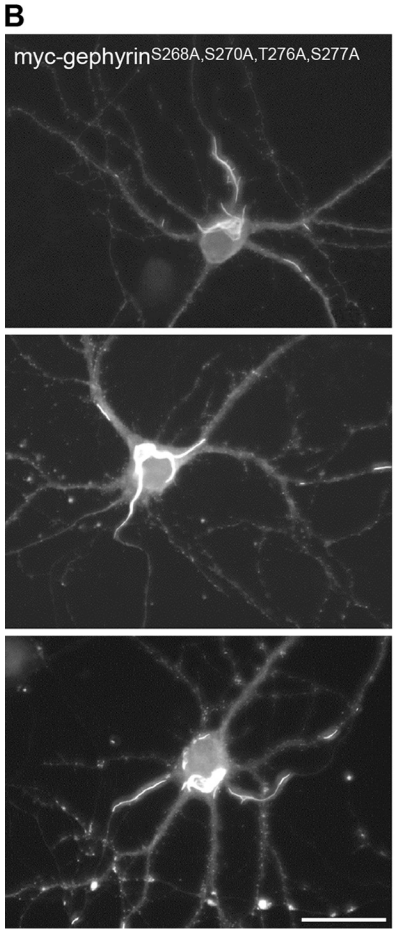
B
myc-gephyrin S268A,S270A,T276A,S277A

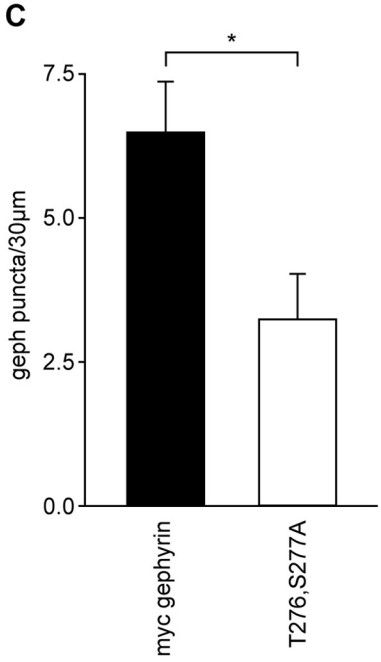
C
*
7.5
5.0
2.5
0.0
geph puncta/30μm
myc gephyrin
T276,S277A

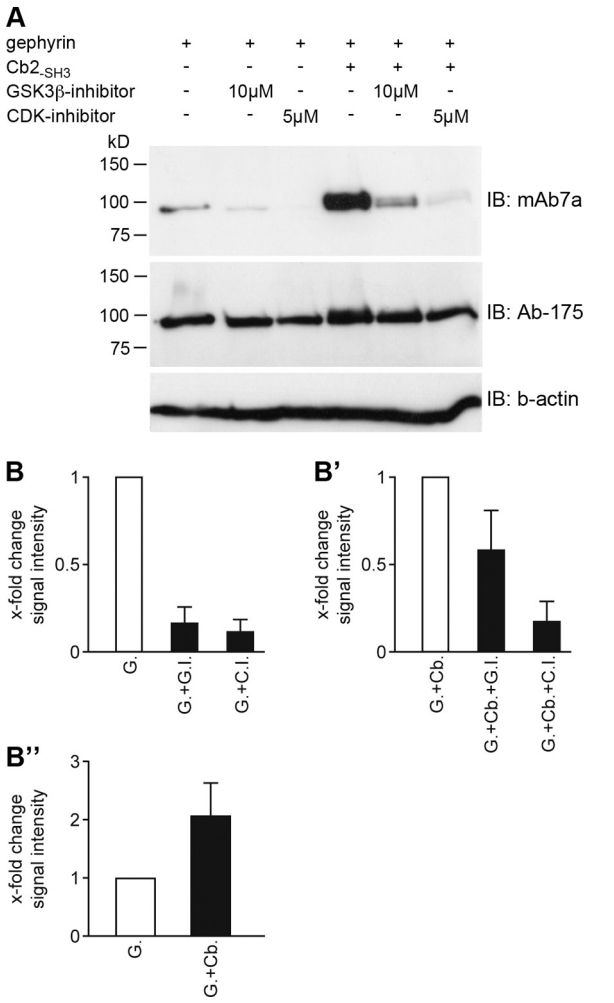


FIGURE 4. **Collybistin coexpression increases kinase-dependent mAb7a immunoreactivity of gephyrin.** *A*, Myc-gephyrin was coexpressed in HEK293T cells with $Cb2_{-SH3}$, and the cell culture medium was supplemented with the indicated GSK3$\beta$ inhibitor (AR-A014418) and CDK inhibitor (aminopurvalanol A) concentrations for 1 day. Cell protein extracts were separated with SDS-PAGE, and the immunoblot (*IB*) was done with mAb7a, Ab-175 antibody, and anti-$\beta$ actin antibody as the loading control. *B*, quantification of mAb7a immunoblot signal intensities upon inhibition of gephyrin expressed alone from three independent experiments is shown. *G*, expression of gephyrin; *G.I.*, GSK3$\beta$ inhibitor; *C.I.*, CDK inhibitor. *B'*, quantification of inhibition upon gephyrin and collybistin ($Cb2_{-SH3}$) coexpression is shown. Data analysis was same as in *B*. *G.+Cb.*, gephyrin and $Cb2_{-SH3}$ coexpression. *B''*, quantification of the difference in signal intensity comparing gephyrin and gephyrin-$Cb2_{-SH3}$ coexpression is shown. Data were corrected for identical gephyrin protein amounts detected with Ab-175 and normalized to mAb7a signal intensity with gephyrin expression. *Error bars* show the mean ± S.D. values.

binding on gephyrin. First, we wanted to directly identify phosphorylation sites of gephyrin by mass spectrometry. For this purpose we purified $His_6$-tagged gephyrin after expression in HEK293T cells in the presence or absence of collybistin ($Cb2_{-SH3}$). With this approach we identified in gephyrin expressed alone the amino acid positions Thr-266, Ser-283, Thr-286, and Ser-295 in the C-domain to be phosphorylated (see Table 1 and supplemental Fig. 2). Interestingly, with gephyrin prepared upon coexpression with $Cb2_{-SH3}$, we identified in addition the positions Ser-268 and Ser-280 to be phosphorylated (see Table 1, supplemental Fig. 2).

**TABLE 1**

**Sequence of identified peptides with mascot ion score and amino acid residues that were identified to be phosphorylated**

Identification of phosphorylated gephyrin peptides is shown. Lowercase letters in the sequence indicate phosphorylated residues (s, t) or cysteine modifications (carbamidomethylation) (c).

| | Peptide | Mascot ion score | Amino acid residue |
|---|---|---|---|
| 1 | R ↓ DTASLSTtPSESPR ↓ A | 69 | Thr-266 |
| 2 | R ↓ DTASLSTTPsESPR ↓ A | 72 | Ser-268 |
| 3 | R ↓ AQATSRLsTAScPTPK ↓ V | 52 | Ser-280 |
| 4 | R ↓ LSTAscPTPK ↓ V | 45 | Ser-283 |
| 5 | R ↓ LSTAScPtPK ↓ V | 49 | Thr-286 |
| 6 | R ↓ cSsKENILR ↓ A | 45 | Ser-295 |

In a second approach to verify phosphorylation as a crucial determinant of mAb7a binding, we applied synthetic peptides in a competition assay. Peptides harbored the gephyrin sequence from position Ala-261 to Ser-283 (ASLSTTPSESPRAQATSRLSTAS) without any phosphorylation or with phosphorylation at either position Ser-268, Ser-270, or Thr-276. After preincubation of mAb7a with these peptides, we applied the antibody in immunoblot assays. As shown in Fig. 5*A*, the peptide phosphorylated at Ser-270 competes with a significantly higher efficacy than the unphosphorylated peptide, resulting in a strongly reduced signal of mAb7a in immunoblots (Fig. 5, *A* and *A'*), establishing that mAb7a is a phospho-dependent antibody sensitive to phosphorylation at position Ser-270. Moreover, peptides that were phosphorylated either at position Ser-268 or Thr-276 did not significantly reduce mAb7a signals compared with the non-phosphorylated peptide. However, upon using higher peptide concentrations (1–2 mg/ml), the nonphosphorylated peptide also competes with gephyrin for mAb7a binding (data not shown), suggesting a low affinity binding. To correlate these data with our mutagenesis data, we analyzed in addition to the gephyrin double mutants (Fig. 2) the single amino acid mutations S268(A/E), S270(A/E), T276(A/E), and S277(A/E) in immunoblots. As shown in Fig. 5, *B* and *C*, only the single mutants S270(A/E) and T276(A/E) revealed strong reduction of mAb7a binding. In addition, the analysis of alanine mutants at positions Thr-266, Ser-280, Ser-283, Thr-286, and Ser-295 identified in mass spectrometry revealed no contribution to mAb7a epitope formation (data not shown). Other, smaller alterations of mAb7a binding with mutants at the flanking positions Ser-268 and Ser-277 (see

FIGURE 3. **A double mutation at Thr-276/Ser-277 reduces myc-gephyrin clusters in hippocampal neurons.** *A'*, immunofluorescence experiments revealed a large degree of overlapping immunoreactivity specific for transiently expressed recombinant myc-gephyrin (*green*), mAb7a puncta (*red*), and $\gamma$2 subunits of $GABA_A$ receptors (*blue*), suggesting that the distribution of recombinant gephyrin is very similar to endogenous gephyrin expressed in hippocampal neurons. *A''*, mutated recombinant gephyrin (S268A,S270A) is colocalized with $GABA_A$ $\gamma$2 subunits receptor clusters in hippocampal neurons. *A'''*, mutation of Thr-276 and Ser-277 to alanine reduced the number of gephyrin clusters. In addition, larger elongated gephyrin structures are formed within the cell body and the dendritic tree, eventually looking like "giant synapse structures." Tee *scale bar* is 30 $\mu$m. *B* shows a similar phenotype of gephyrin localization as seen in Fig. *A'''* for cells expressing the mutant $gephyrin^{S268A,S270A,T276A,S277A}$ with three example cells. The *scale bar* is 30 $\mu$m. *C*, quantification of gephyrin cluster numbers expressing wild-type gephyrin and $gephyrin^{T276A,S277A}$ is shown. Cluster number was estimated for three dendritic segments of 30-$\mu$m length from 12–15 cells derived from three independent cultures. *Error bars* show mean ± S.E. values. The *asterisk* indicates $p < 0.05$ in Student's *t* test and is regarded as significant.

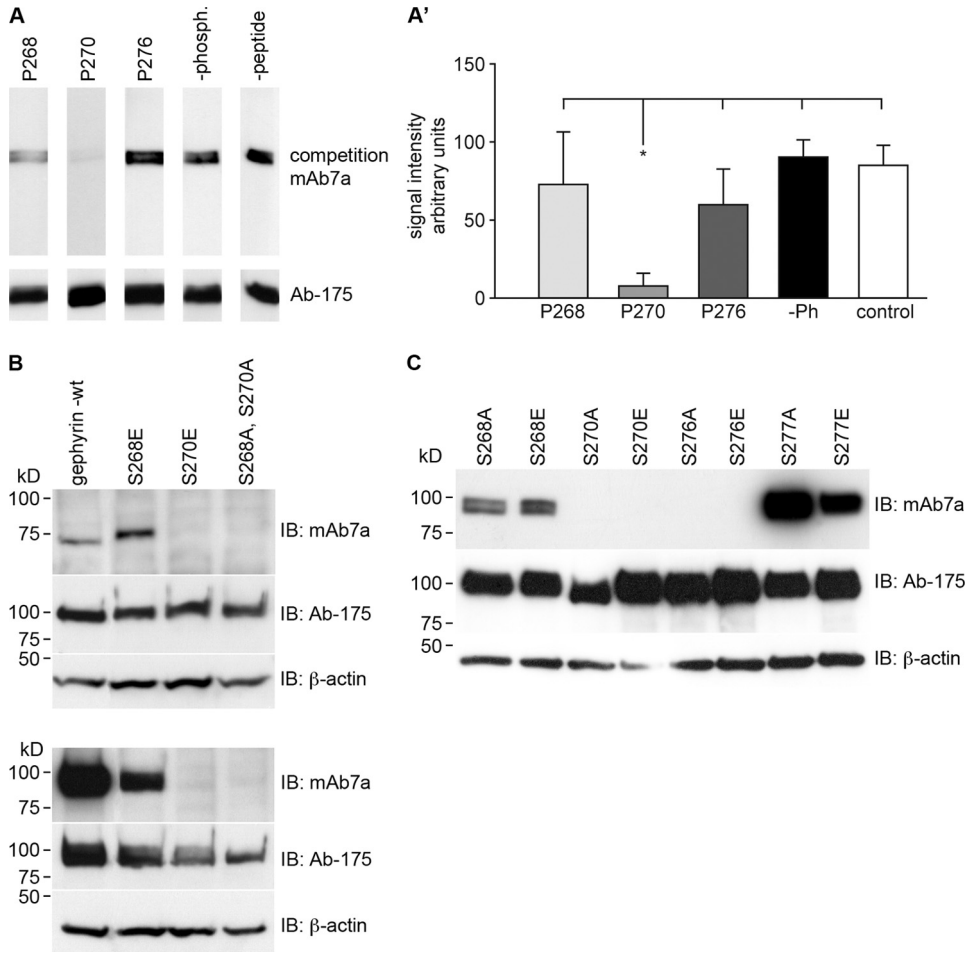


FIGURE 5. **mAb7 epitope characterization.** *A*, peptides with phosphates at position Ser-268 (*P268*), Ser-270 (*P270*), or Thr-276 (*P276*) and non-phosphate peptide (−*phosph.*) with a concentration of 0.25 mg/ml were preincubated with mAb7a and applied for immunoblot analysis with membrane-bound gephyrin. The same stripes as above were stained with Ab-175. *A'*, quantification of immunoblot signal intensities is shown. Quantification was done from the results from three to six (P270) independent experiments. Data show the mean ± S.D. values. *p* values of $p < 0.05$ (*) were regarded as significant. Immunoblot analysis of gephyrin mutants is shown. *B*, *upper panel*, glutamate mutations of Ser-268 or Ser-270 were compared with double mutant gephyrin$^{S268AS270A}$ or gephyrin wild type upon single expression in HEK293T. *Lower panel*, shown are immunoblots (*IB*) of the same gephyrin variants as in the *upper panel* upon coexpression with $Cb2_{-SH3}$. *C*, Myc-gephyrin- or a $His_6$-gephyrin-mutants (S270A) were coexpressed with $Cb2_{-SH3}$ in HEK293T cells. After 2 days protein extracts were prepared and analyzed in immunoblots with mAb7a or Ab-175. Blots show representative results from three to five independent experiments.

Fig. 5*C*) might be indirect effects onto the amino acid positions Ser-270 and Thr-276 or may indicate some minor direct contribution to the antibody binding, an open question that might be addressed in future studies. Taken together, these experiments disclosed that high affinity binding of mAb7a to gephyrin is dependent on the amino acid side chain at position Thr-276 and on phosphorylation at position Ser-270.

*CDKs Are Involved in Phosphorylation of Gephyrin in Hippocampal Neurons*—Our inhibition experiments (Fig. 4) showed that CDKs are involved in phosphorylation of gephyrin in HEK293T cells. As CDK5 is well established to play an important role in regulating different aspects of synaptic plasticity of excitatory synapses (35), we asked whether CDKs might also be involved in phosphorylation of gephyrin in neurons.

We applied CDK inhibitor aminopurvalanol A (0.8 or 1 $\mu$M) to cultured hippocampal neurons for 3, 4, or 7 days and determined the number of mAb7a immunoreactive puncta. As shown in Fig. 6, this treatment resulted in a significant decrease of the number of mAb7a puncta with 1 $\mu$M for 4 day or for 0.8 and 1 $\mu$M for 7 days of treatment (Fig. 6*A*) (see also supplemental Fig. 1). To determine the minimal concentration of inhibitor necessary to induce a reduction in immunoreactivity, we applied aminopurvalanol A from 40 nM to 1 $\mu$M concentrations for 7 days. These experiments showed that the decrease of number and size of clusters was dose-dependent. As shown in Fig. 6*B*, aminopurvalanol A concentrations ≥0.4 $\mu$M already resulted in a significant reduction of mAb7a puncta numbers. About 75% reduction was achieved with 1 $\mu$M aminopurvalanol A (4.23 ± 0.36 puncta/30 $\mu$m in DMSO-treated neurons (D) and 0.92 ± 0.34 puncta/30 $\mu$m with 1 $\mu$M amino-purvalanol A.; mean ± S.E.). In addition, the size of puncta was reduced from 0.48 ± 0.14 $\mu m^2$ to 0.17 ± 0.06 $\mu m^2$ upon treatment with 1 $\mu$M aminopurvalanol A (mean ± S.E.) (Fig. 6*C*). Comparing the number and size of VIAAT clusters with 1 $\mu$M aminopurvalanol A concentrations and DMSO control, we could show that this treatment had no significant impact on VIAAT immunofluorescence signals (Fig. 6, *D* and *E*).

Next, we investigated which effect the application of aminopurvalanol A might have on later stages of *in vitro* differentia-

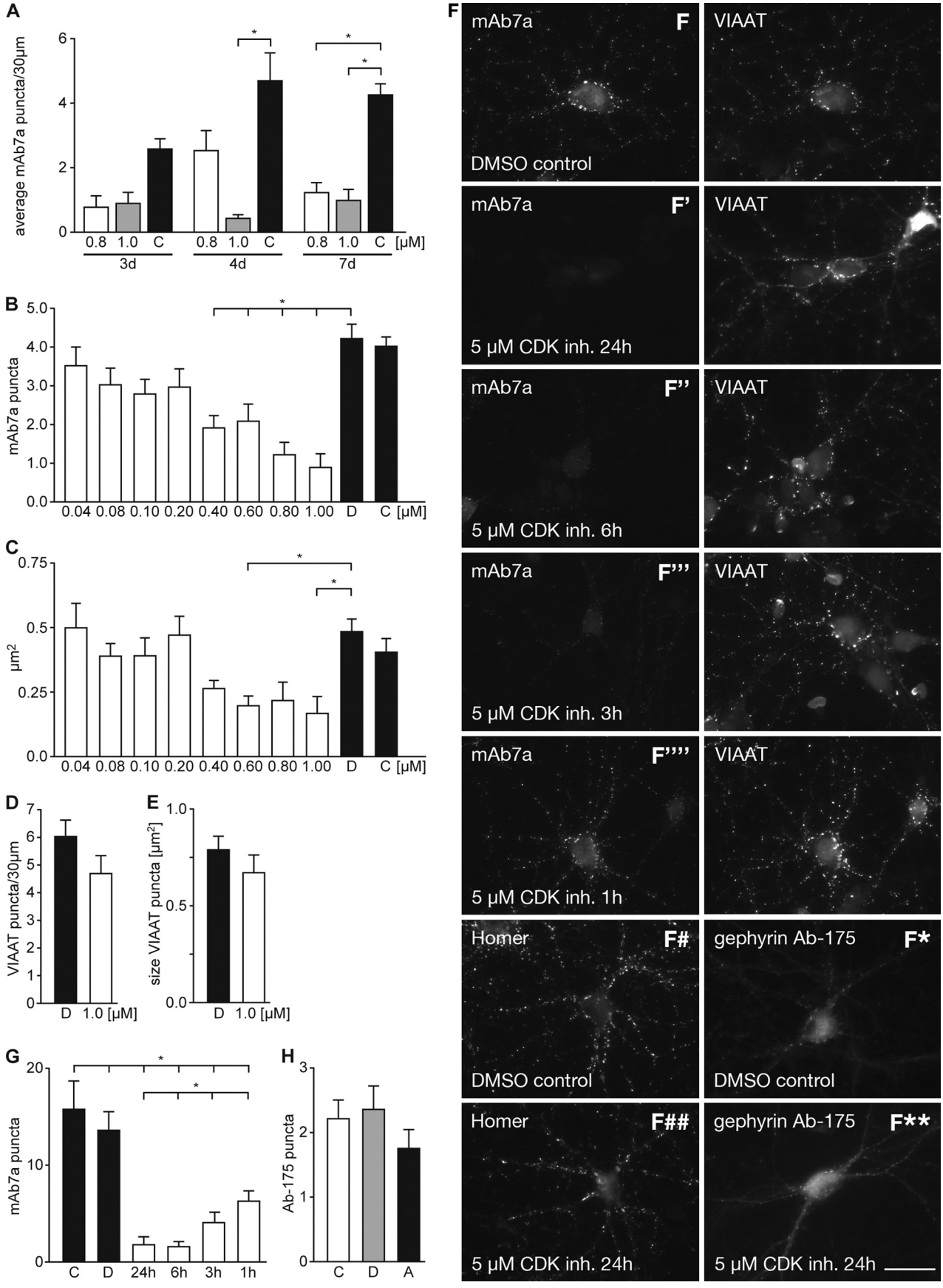
A
average mAb7a puncta/30µm
0.8 1.0 C 0.8 1.0 C 0.8 1.0 C [µM]
3d
4d
7d
B
mAb7a puncta
0.04 0.08 0.10 0.20 0.40 0.60 0.80 1.00 D C [µM]
C
µm²
0.04 0.08 0.10 0.20 0.40 0.60 0.80 1.00 D C [µM]
D
VIAAT puncta/30µm
D 1.0 [µM]
E
size VIAAT puncta [µm²]
D 1.0 [µM]
G
mAb7a puncta
C D 24h 6h 3h 1h
H
Ab-175 puncta
C D A
F
mAb7a F
VIAAT
DMSO control
mAb7a F'
VIAAT
5 µM CDK inh. 24h
mAb7a F''
VIAAT
5 µM CDK inh. 6h
mAb7a F'''
VIAAT
5 µM CDK inh. 3h
mAb7a F''''
VIAAT
5 µM CDK inh. 1h
Homer F#
gephyrin Ab-175 F*
DMSO control
DMSO control
Homer F##
gephyrin Ab-175 F**
5 µM CDK inh. 24h
5 µM CDK inh. 24h

tion, when synaptic structures are more developed and the CDK inhibitor is applied for shorter time periods. We applied 5 $\mu$M aminopurvalanol A at div13 and div14 for 24, 6, 3, and 1 h before fixation of the cells. As shown in Fig. 6*F*, mAb7a immunoreactivity is strongly reduced in cultures with CDK inhibition for 24 h (Fig. 6*F′*). Also 6-h (*F″*), 3-h (*F‴*), and 1-h treatments revealed significant reduction of mAb7a staining (Fig. 6*G*). For comparison, we stained neurons treated for 24 h with 5 $\mu$M aminopurvalanol A for the presynaptic markers VIAAT and the excitatory synapse marker protein Homer. We did not detect strong alteration in staining of these proteins (Fig. 6*F*, # and ##). Moreover, staining of cultures that were treated for 24 h with 5 $\mu$M aminopurvalanol A with the gephyrin-specific antibody Ab-175 showed that the cluster number and size detected with Ab-175 was not altered in the same way as mAb7a stainings (Fig. 6*F*, * and **), revealing that reduced phosphorylation of gephyrin at position Ser-270 at established postsynaptic structures is not correlated with a reduction of the gephyrin scaffold during the time period of 1–24 h.

We did also stainings at div9 stages with Ab-175 after treatment with 0.8 $\mu$M aminopurvalanol A for 4 days. Unexpectedly, Ab-175 immunoreactivity was not significantly reduced (Fig. 6*H*), suggesting that alterations of mAb7a immunoreactivity does not imply changes in the gephyrin scaffold detected by Ab-175. Thus future experiments have to disclose which functional impact phosphorylation at Ser-270 for cluster formation might have.

Aminopurvalanol A is known to inhibit different CDKs with similar affinities, as $IC_{50}$ values are 33, 28, and 20 nM for CDK1/cyclinB, CDK2/cyclinE, and CDK5/p35, respectively, for *in vitro* kinase activity. To investigate which of these kinases was involved in the phosphorylation of gephyrin as monitored by mAb7a immunoreactivity, we chose *in vitro* phosphorylation assays with purified gephyrin and purified enzymes.

Purified N-terminal $His_6$-tagged gephyrin was incubated with CDK1/cyclinB complexes or CDK2/cyclinA or CDK5/p25NCK in the presence of ATP and analyzed by mAb7a immunoblots. As shown in Fig. 7, *A–D″*, mAb7a immunoreactivities were clearly increased in the presence of increasing activity of CDK1, CDK2, or CDK5 and were strictly dependent on the presence of $Mg^{2+}$ and ATP, indicating that these kinases could phosphorylate gephyrin at Ser-270, which determines the phospho-specific mAb7a sensitivity.

To demonstrate more directly the incorporation of phosphates into gephyrin, we performed the *in vitro* phosphorylation assays also in the presence of [$\gamma$-$^{32}$P]ATP. Interestingly, CDK1, CDK2, and CDK5 all incorporated $^{32}$P into gephyrin (Fig. 7*E*), and the inhibition of the reaction with aminopurvalanol A demonstrated that this phosphorylation was CDK-dependent and not due to a contaminating other kinase activity. Thus, the incorporation of radioactively labeled phosphate into gephyrin more directly shows the phosphorylation of gephyrin by CDKs. Because the putative co-immunoprecipitation of CDK5 in the *in vitro* phosphorylation assay (Fig. 7*E*) indicates a binding of CDK5 to gephyrin, we performed immunoprecipitation of CDK5 with protein extracts from cultured neurons. As shown in Fig. 7*F*, incubation of protein extracts with a CDK5-specific antibody, but not with an unrelated control antibody, allowed the co-precipitation of gephyrin from cultured rat hippocampal and spinal cord neurons, suggesting that these experiments identified CDK5 as a novel binding protein of gephyrin in neurons.

## DISCUSSION

The data presented in this paper provide novel information for understanding the gephyrin-dependent formation of GlyR and $GABA_A$ receptor clusters at postsynaptic membrane specializations. First, we demonstrate for the first time that Cb affects the phosphorylation of gephyrin. Second, we show that phosphorylation of gephyrin at position Ser-270 can be detected using the monoclonal antibody mAb7a. Third, we identify CDK5 as novel binding protein of gephyrin and provide evidence that CDK5 and other related CDKs may be involved in the phosphorylation of gephyrin at position Ser-270.

We performed shRNA-mediated Cb knockdown experiments that resulted in a robust reduction of mAb7a immunoreactivity at postsynaptic sites, suggesting an almost complete loss of gephyrin clusters in most infected neurons. Immunoblot analysis revealed that the loss of mAb7a immunoreactivity was not due to a reduction of total gephyrin protein expression, as the use of antibody Ab-175 revealed comparable gephyrin levels in control and Cb knockdown cell cultures. Dephosphorylation experiments showed that mAb7a immunoreactivity was dependent on the phosphorylation of gephyrin. This finding is supported by the fact that mutation of one putative phosphorylation site (Ser-270) abolished mAb7a immunoreactivity. In addition, the inhibition of different kinase pathways in HEK293T cells expressing gephyrin and Cb resulted in a strong reduction of mAb7a binding to gephyrin, demonstrating that mAb7a detects kinase-dependent phosphorylation of gephyrin. Moreover, the coexpression of gephyrin with $Cb2_{-SH3}$ strongly increased the mAb7a-specific signals in immunoblots, supporting our hypothesis that the phosphorylation of gephyrin is dependent on the presence of Cb. Interestingly, in 2000, Kins *et*

FIGURE 6. **Pharmacological inhibition of kinases in hippocampal neurons reduces mAb7a puncta.** *A*, supplementation of the cell culture medium with aminopurvalanol A (0.8 and 1 $\mu$M) for three (*3d*), four (*4d*), or 7 days (*7d*) reduced mAb7a puncta number at day 9. *B*, dose-dependent reduction of VIAAT apposed mAb7a clusters at div9 upon incubation of hippocampal neurons for 7 days with aminopurvalanol A concentrations ranging from 0.04 to 1 $\mu$M. *C*, dose-dependent reduction of mAb7a cluster sizes at div9 upon the same treatment as in *B*. *D*, shown is quantification of VIAAT cluster numbers upon CDK inhibition for 7 days. *E*, quantification of VIAAT cluster sizes upon CDK inhibition for 7 days. Cluster number and cluster sizes were estimated for three dendritic segments of 30 $\mu$m in length of 8–10 cells from three independent cultures in blinded analysis. *Error bars* show the mean ± S.E. values. * indicates $p < 0.05$ in analysis of variance and was regarded as significant. *F*, inhibition of CDKs with aminopurvalanol A (5 $\mu$M) for 24 h (F′), 6 h (F″), 3 h (F‴), or 1 h (F‴ ′) at div14 is shown. Cells were stained with mAb7a and anti-VIAAT antibody, with anti-Homer (*F*, # and ##) or with the gephyrin antibody Ab-175 (*F*, * and **). *G*, shown is quantification of reduced mAb7a puncta upon 1–24 h aminopurvalanol A treatment. *Error bars* show mean ± S.E. values from three independent experiments ($n = 15$). *, indicates $p < 0.05$ in one way analysis of variance and was regarded as significant. *H*, shown is quantification of Ab-175 puncta upon 4 days of 0.8 $\mu$M aminopurvalanol A treatment. *D*, DMSO; *C*, control; *A*, aminopurvalanol A. *Error bars* show mean ± S.E. values from three independent experiments ($n$ = 15–30).

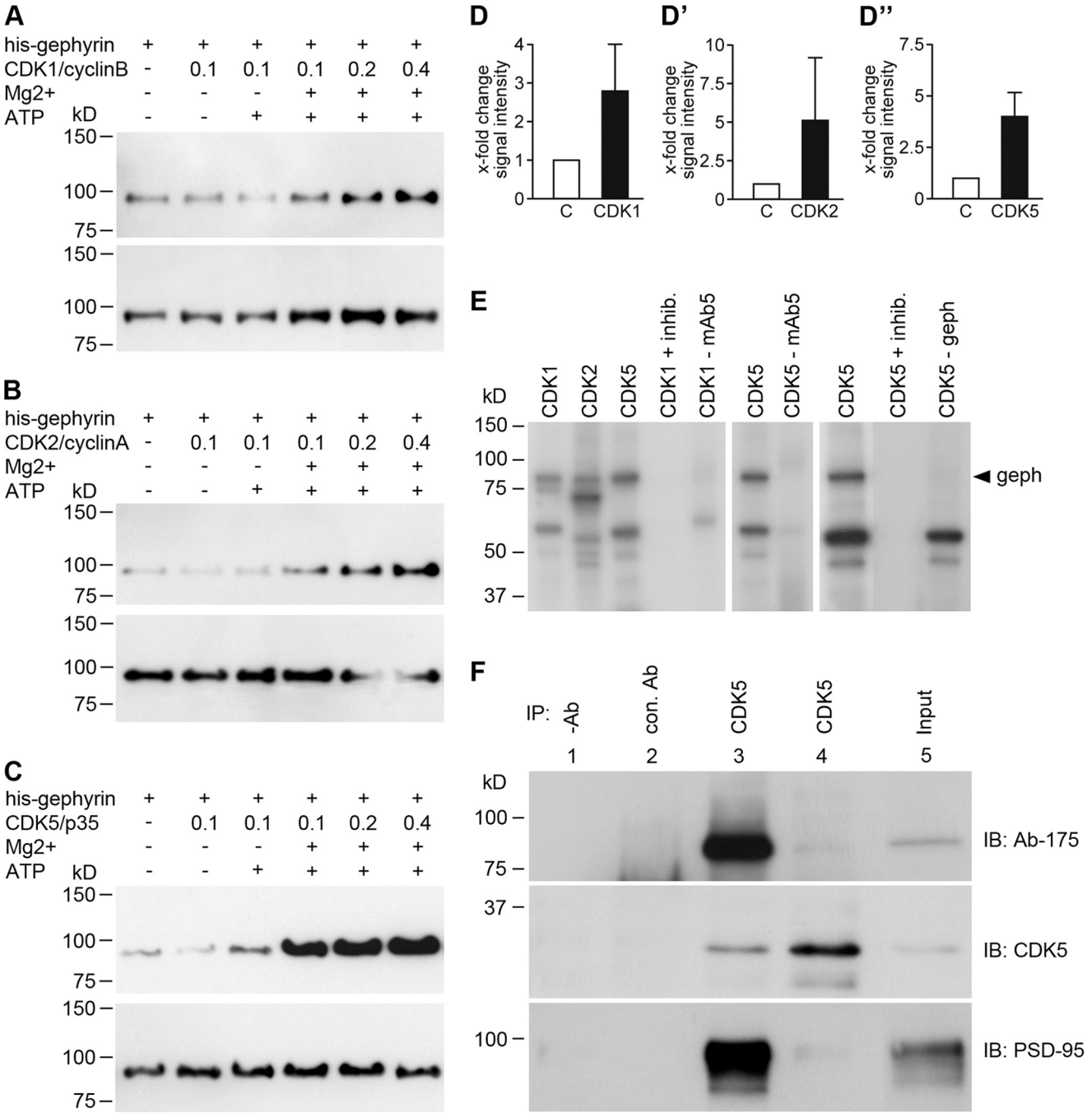


FIGURE 7. ***In vitro* phosphorylation assays revealed phosphorylation of gephyrin by CDKs.** Purified $His_6$-gephyrin was incubated with purified CDK1/cyclinB (*A*), CDK2/cyclinA (*B*), and CDK5/p25NCK (*C*) complexes, and proteins were analyzed in immunoblot experiments with mAb7a (*upper panel*) and Ab-175 antibody (*lower panel*). In the presence of CDK1/cyclinB, CDK2/cyclinA and CDK5/p25NCK mAb7a signal intensities were increased. *D*, quantification of immunoblot intensities is shown. Shown is a comparison of assays without ATP/$Mg^{2+}$ (*C*) and with ATP and $Mg^{2+}$ and 0.2 unit of CDK enzymes (*CDK*). *Bars* show the mean ± S.D. values. mAb7a mean pixel intensities were corrected for same protein amounts detected with Ab-175 and were normalized to values of gephyrin without CDKs activity. *E*, shown is incorporation of radioactively labeled phosphate in gephyrin by CDK1, -2, and -5. Besides the labeling of gephyrin, lower molecular weight bands revealed $^{32}P$ incorporation in the absence of gephyrin (*CDK5-geph*), suggesting that these proteins might be the GST-CDK1/2/5 fusion proteins that are co-immunoprecipitated. Note that the labeled gephyrin is not detected in experiments lacking mAb5 (*CDK-mAb5*). *F*, co-immunoprecipitation (*IP*) of CDK5 and gephyrin from neuronal protein extracts is shown. Co-precipitation of gephyrin upon CDK5 immunoprecipitation from protein extracts from cultured hippocampal (div21) (*lane 3*) and spinal cord (div21) (*lane 4*) neurons is shown. Gephyrin was detected with Ab-175. Controls are the assay without antibody (*lane 1*) or with an unrelated antibody (*lane 2*). The input (*lane 5*) was loaded with 20% of the amount of extract used for immunoprecipitation. Note, as the control, PSD-95 is also co-precipitated, confirming published data (34). The figure shows a representative result from three independent experiments.

*al.* (3) showed that coexpression of $Cb2_{-SH3}$ with gephyrin in HEK293 cells induced the formation of submembranous gephyrin microclusters instead of gephyrin "blobs" which were observed upon expression of gephyrin alone. Thus, future experiments have to disclose whether these observations are functionally related.

Besides the strong increase in mAb7a immunoreactivity upon coexpression of gephyrin with $Cb2_{-SH3}$, the migration

behavior of gephyrin in SDS-PAGE was also altered. One single band was detected with increasing intensity, whereas a second, slower migrating band appeared in addition when comparing the single expression of gephyrin with coexpression of gephyrin and $Cb2_{-SH3}$ (see Fig. 4). As the reduction of mAb7a immunoreactivity of both bands was observed in neurons upon Cb knockdown, these results support the view that one functional role of collybistin is to mediate the phosphorylation of gephyrin by one or more different kinases and that gephyrin may exist in at least two different forms resulting from post-translational modifications.

The use of different kinase inhibitors in HEK293T expression experiments showed that kinases like GSK3$\beta$ and CDKs might be involved in the phosphorylation of gephyrin. Pharmacological inhibition of CDKs in cultured hippocampal neurons resulted in the reduction of mAb7a puncta upon prolonged inhibition at div9, whereas the general staining pattern of presynaptic markers from inhibitory synapses (VIAAT) or postsynaptic markers from excitatory synapses (PSD95, Homer) were not altered. However, the results using another antibody (Ab-175) specific for gephyrin were different. Although the mean values of the number of gephyrin puncta were reduced, this reduction did not reach significance levels. Therefore, it might be possible that the formation or stability of gephyrin clusters is independent of CDK-mediated phosphorylation. On the other hand, one might speculate that the remaining phosphorylation of gephyrin under our experimental conditions was sufficient to allow gephyrin cluster formation.

In addition, we demonstrated that shorter incubation (1–6 h) with higher concentrations of inhibitors reduced mAb7a-specific puncta at div14 stages. Again this reduction of mAb7a immunoreactivity is not correlated with a similar decrease of Ab-175 immunoreactivity, suggesting that dephosphorylation of existing gephyrin clusters may reduce mAb7a immunoreactivity. Alternatively, it may be possible that mAb7a clusters have a short half-life and the turn-over of gephyrin at existing clusters is independent of CDK-mediated phosphorylation. From our inhibition experiments, we conclude that the reduced phosphorylation of gephyrin at position Ser-270 in Cb knockdown hippocampal neurons may not play a major role for the reduction of gephyrin clusters (see also Ref. 30). However, other functional roles like alteration in gephyrin-receptor interactions, ion channel behavior, or "cellular signaling" of gephyrin receptor complexes (16) depending on phosphorylation at Ser-270 of gephyrin might be possible.

The hypothesis that CDKs are involved in the phosphorylation of gephyrin is further supported by the results of *in vitro* phosphorylation assays. Using purified recombinant gephyrin to perform *in vitro* assays with recombinant CDK1/cyclinB, CDK2/cyclin A, or CDK5/p25NCK complexes resulted in an increase in mAb7a immunoreactivity as detected by immunoblot analysis. Moreover, a direct incorporation of radioactively labeled phosphate was demonstrated. Using phosphorylation prediction algorithms for the sequence of the C-domain, several sites are indicated to be putative phosphorylation sites of CDK1 or CDK5 (NetPhosK 1.0 Server). Interestingly, the positions Ser-270 as well as Thr-276 and Ser-277 were predicted as putative CDK sites in gephyrin. Using peptide competition experiments, we confirmed that mAb7a binding to peptides phosphorylated at Ser-270 was stronger than binding to the unphosphorylated peptide, thus indicating that mAb7a puncta detected in fluorescence microscopy are indeed composed of gephyrin, which are phosphorylated at position Ser-270. Mass spectrometry analysis identified position Ser-268 to be phosphorylated in addition to five other positions within the C-domain of gephyrin. Future experiments expressing respective gephyrin mutants in neurons with a gephyrin knock-out genotype may allow disclosure of the putative function of these phosphorylation sites.

Studies in other laboratories have shown that inhibition of phosphatase 1 decreased gephyrin cluster size (25) and that inhibition of GSK3$\beta$ kinase with high $Li^{2+}$ concentrations increased gephyrin clustering (24), and these findings indicated that dephosphorylation of gephyrin at Ser-270 supports cluster formation, suggesting that mature gephyrin clusters might not be phosphorylated at Ser-270. However, our data indicate that phosphorylation of gephyrin at position Ser-270 is essential for gephyrin cluster detection with mAb7a. As it was shown that the phosphorylation by GSK3$\beta$ at Ser-270 limits cluster formation (24) and our study disclosed that mutations at the neighbored position 276/277 induced the formation of giant cluster-like structures in dendrites, one might speculate that this gephyrin domain is involved in restricting the polymerization of gephyrin scaffolds.

Moreover, we cannot exclude that the gephyrin scaffolds at the postsynaptic membrane are not homogenous in respect of gephyrin modifications. Instead, the assembly from at least two different conformations or states of gephyrin seems possible, as indicated by the presence of two different migrating gephyrin bands from protein extracts of cultured neurons or upon coexpressing gephyrin with $Cb2_{-SH3}$ in heterologous cells. Thus, one might speculate that gephyrin scaffolds *in vivo* are composed of a specific mixture of phosphorylated and nonphosphorylated gephyrin at a given site.

The hypothesis that the long and curving gephyrin structures upon expressing $gephyrin^{S268A,S270A,T276A,S277A}$ reflect an unrestricted oligomerization behavior of gephyrin is in agreement with the description of very similar structures in hippocampal neurons expressing a collybistin impaired in the PH domain (26). Interestingly, the gephyrin phenotype in that study was rescued by the coexpression of constitutively active Cdc42. It is, therefore, possible that Cdc42 in those experiments might have activated downstream pathways converging to processes that involve the gephyrin region around Ser-270/Thr-276/Ser-277. The striking "needle" gephyrin phenotype might be related to unrestricted oligomerization behavior dependent on specific gephyrin conformations or interaction with additional proteins.

Our finding that CDK1 might be a kinase involved in phosphorylation of gephyrin was unexpected. In contrast to CDK5 (35), only few data are available concerning the function of CDK1 in postmitotic neurons. Recently, a study reported the association of CDK1 with the microtubule network and the tubulin-binding protein tau in postmitotic neurons (36). Our

data suggest that either CDK1, CDK2, or CDK5 could phosphorylate gephyrin; however, the identification of CDK5 as a gephyrin-binding protein by co-immunoprecipitation experiments suggests that CDK5 is a major candidate as a kinase expressed in postmitotic neurons to phosphorylate gephyrin. Future experiments have to establish which of the identified sites beside Ser-270 are phosphorylated by CDK5 or the other CDKs *in vivo*. In addition, the functional role of Cb for the phosphorylation of gephyrin and its functional impact in neuronal functions has to be elucidated by further *in vitro* and *in vivo* experiments.

*Acknowledgments—We thank Rita Rossner for excellent technical assistance, Prof. Dr. K. Gorgas for reading the manuscript, M. Kaiser for providing the Cb2$_{-SH3}$ rescue construct, R. Nonnenmacher for figure lay out, and P. Meller and N. Nierobisch for excellent technical assistance. Mass spectrometry was performed from the Core Facility for Mass Spectrometry and Proteomics, ZMBH, University Heidelberg.*

## REFERENCES

1. Feng, G., Tintrup, H., Kirsch, J., Nichol, M. C., Kuhse, J., Betz, H., and Sanes, J. R (1998) Dual requirement for gephyrin in glycine receptor clustering and molybdoenzyme activity. *Science* **282,** 1321–1324
2. Kirsch, J., and Betz, H. (1995) The postsynaptic localization of the glycine receptor-associated protein gephyrin is regulated by the cytoskeleton. *J. Neurosci.* **15,** 4148–4156
3. Kins, S., Betz, H., and Kirsch, J. (2000) Collybistin, a newly identified brain-specific GEF, induces submembrane clustering of gephyrin. *Nat. Neurosci.* **3,** 22–29
4. Harvey, K., Duguid, I. C., Alldred, M. J., Beatty, S. E., Ward, H., Keep, N. H., Lingenfelter, S. E., Pearce, B. R., Lundgren, J., Owen, M. J., Smart, T. G., Lüscher, B., Rees, M. I., and Harvey, R. J. (2004) The GDP-GTP exchange factor collybistin. An essential determinant of neuronal gephyrin clustering. *J. Neurosci.* **24,** 5816–5826
5. Poulopoulos, A., Aramuni, G., Meyer, G., Soykan, T., Hoon, M., Papadopoulos, T., Zhang, M., Paarmann, I., Fuchs, C., Harvey, K., Jedlicka, P., Schwarzacher, S. W., Betz, H., Harvey, R. J., Brose, N., Zhang, W., and Varoqueaux, F. (2009) Neuroligin 2 drives postsynaptic assembly at perisomatic inhibitory synapses through gephyrin and collybistin. *Neuron* **63,** 628–642
6. Papadopoulos, T., Korte, M., Eulenburg, V., Kubota, H., Retiounskaia, M., Harvey, R. J., Harvey, K., O'Sullivan, G. A., Laube, B., Hülsmann, S., Geiger, J. R., and Betz, H. (2007) Impaired GABAergic transmission and altered hippocampal synaptic plasticity in collybistin-deficient mice. *EMBO J.* **26,** 3888–3899
7. Papadopoulos, T., and Soykan, T. (2011) The role of collybistin in gephyrin clustering at inhibitory synapses. Facts and open questions. *Front. Cell. Neurosci.* **5,** 11
8. Shimojima, K., Sugawara, M., Shichiji, M., Mukaida, S., Takayama, R., Imai, K., and Yamamoto, T. (2011) Loss-of-function mutation of collybistin is responsible for X-linked mental retardation associated with epilepsy. *J. Hum. Genet.* **56,** 561–565
9. Reddy-Alla, S., Schmitt, B., Birkenfeld, J., Eulenburg, V., Dutertre, S., Böhringer, C., Götz, M., Betz, H., and Papadopoulos, T. (2010) PH-domain-driven targeting of collybistin but not Cdc42 activation is required for synaptic gephyrin clustering. *Eur. J. Neurosci.* **31,** 1173–1184
10. Sola, M., Bavro, V. N., Timmins, J., Franz, T., Ricard-Blum, S., Schoehn, G., Ruigrok, R. W., Paarmann, I., Saiyed, T., O'Sullivan, G. A., Schmitt, B., Betz, H., and Weissenhorn, W. (2004) Structural basis of dynamic glycine receptor clustering by gephyrin. *EMBO J.* **23,** 2510–2519
11. Fritschy, J. M., Harvey, R. J., and Schwarz, G. (2008) Gephyrin. Where do we stand, where do we go? *Trends Neurosci.* **31,** 257–264
12. Betz, H., Kuhse, J., Schmieden, V., Laube, B., Kirsch, J., and Harvey, R. J. (1999) Structure and functions of inhibitory and excitatory glycine receptors. *Ann. N.Y. Acad. Sci.* **868,** 667–676
13. Luscher, B., Fuchs, T., and Kilpatrick, C. L. (2011) GABAA receptor trafficking-mediated plasticity of inhibitory synapses. *Neuron* **70,** 385–409
14. Meyer, G., Kirsch, J., Betz, H., and Langosch, D. (1995) Identification of a gephyrin binding motif on the glycine receptor beta subunit. *Neuron* **15,** 563–572
15. Kirsch, J., Kuhse, J., and Betz, H. (1995) Targeting of glycine receptor subunits to gephyrin-rich domains in transfected human embryonic kidney cells. *Mol. Cell. Neurosci.* **6,** 450–461
16. Bluem, R., Schmidt, E., Corvey, C., Karas, M., Schlicksupp, A., Kirsch, J., and Kuhse, J. (2007) Components of the translational machinery are associated with juvenile glycine receptors and are redistributed to the cytoskeleton upon aging and synaptic activity. *J. Biol. Chem.* **282,** 37783–37793
17. Schrader, N., Kim, E. Y., Winking, J., Paulukat, J., Schindelin, H., and Schwarz, G. (2004) Biochemical characterization of the high affinity binding between the glycine receptor and gephyrin. *J. Biol. Chem.* **279,** 18733–18741
18. Kim, E. Y., Schrader, N., Smolinsky, B., Bedet, C., Vannier, C., Schwarz, G., and Schindelin, H. (2006) Deciphering the structural framework of glycine receptor anchoring by gephyrin. *EMBO J.* **25,** 1385–1395
19. Tretter, V., Jacob, T. C., Mukherjee, J., Fritschy, J. M., Pangalos, M. N., and Moss, S. J. (2008) The clustering of GABA(A) receptor subtypes at inhibitory synapses is facilitated via the direct binding of receptor $\alpha$2 subunits to gephyrin. *J. Neurosci.* **28,** 1356–1365
20. Saiepour, L., Fuchs, C., Patrizi, A., Sassoè-Pognetto, M., Harvey, R. J., and Harvey, K. (2010) Complex role of collybistin and gephyrin in GABAA receptor clustering. *J. Biol. Chem.* **285,** 29623–29631
21. Maric, H. M., Mukherjee, J., Tretter, V., Moss, S. J., and Schindelin, H. (2011) Gephyrin-mediated GABA(A) and glycine receptor clustering relies on a common binding site. *J. Biol. Chem.* **286,** 42105–42114
22. Langosch, D., Hoch, W., and Betz, H. (1992) The 93 kDa protein gephyrin and tubulin associated with the inhibitory glycine receptor are phosphorylated by an endogenous protein kinase. *FEBS Lett.* **298,** 113–117
23. Zita, M. M., Marchionni, I., Bottos, E., Righi, M., Del Sal, G., Cherubini, E., and Zacchi, P. (2007) Post-phosphorylation prolyl isomerization of gephyrin represents a mechanism to modulate glycine receptors function. *EMBO J.* **26,** 1761–1771
24. Tyagarajan, S. K., Ghosh, H., Yévenes, G. E., Nikonenko, I., Ebeling, C., Schwerdel, C., Sidler, C., Zeilhofer, H. U., Gerrits, B., Muller, D., and Fritschy, J. M. (2011) Regulation of GABAergic synapse formation and plasticity by GSK3beta-dependent phosphorylation of gephyrin. *Proc. Natl. Acad. Sci. U.S.A.* **108,** 379–384
25. Bausen, M., Weltzien, F., Betz, H., and O'Sullivan, G. A. (2010) Regulation of postsynaptic gephyrin cluster size by protein phosphatase 1. *Mol. Cell. Neurosci.* **44,** 201–209
26. Tyagarajan, S. K., Ghosh, H., Harvey, K., and Fritschy, J. M. (2011) Collybistin splice variants differentially interact with gephyrin and Cdc42 to regulate gephyrin clustering at GABAergic synapses. *J. Cell Sci.* **124,** 2786–2796
27. Pfeiffer, F., Simler, R., Grenningloh, G., and Betz, H. (1984) Monoclonal antibodies and peptide mapping reveal structural similarities between the subunits of the glycine receptor of rat spinal cord. *Proc. Natl. Acad. Sci. U.S.A.* **81,** 7224–7227
28. Prior, P., Schmitt, B., Grenningloh, G., Pribilla, I., Multhaup, G., Beyreuther, K., Maulet, Y., Werner, P., Langosch, D., and Kirsch, J. (1992) Primary structure and alternative splice variants of gephyrin, a putative glycine receptor-tubulin linker protein. *Neuron* **8,** 1161–1170
29. Lois, C., Hong, E. J., Pease, S., Brown, E. J., and Baltimore, D. (2002) Germline transmission and tissue-specific expression of transgenes delivered by lentiviral vectors. *Science* **295,** 868–872
30. Körber, C., Richter, A., Kaiser, M., Schlicksupp, A., Mükusch, S., Kuner, T., Kirsch, J., and Kuhse, J. (2012) Effects of distinct collybistin isoforms on the formation of GABAergic synapses in hippocampal neurons. *Mol. Cell. Neurosci.* **50,** 250–259
31. Dresbach, T., Hempelmann, A., Spilker, C., tom Dieck, S., Altrock, W. D., Zuschratter, W., Garner, C. C., and Gundelfinger, E. D. (2003) Functional

regions of the presynaptic cytomatrix protein bassoon. Significance for synaptic targeting and cytomatrix anchoring. *Mol. Cell. Neurosci.* **23,** 279–291
32. Nawrotzki, R., Islinger, M., Vogel, I., Völkl, A., and Kirsch, J. (2012) Expression and subcellular distribution of gephyrin in non-neuronal tissues and cells. *Histochem. Cell Biol.* **137,** 471–482
33. Dephoure, N., Zhou, C., Villén, J., Beausoleil, S. A., Bakalarski, C. E., Elledge, S. J., and Gygi, S. P. (2008) A quantitative atlas of mitotic phosphorylation. *Proc. Natl. Acad. Sci. U.S.A.* **105,** 10762–10767
34. Morabito, M. A., Sheng, M., and Tsai, L. H. (2004) Cyclin-dependent kinase 5 phosphorylates the N-terminal domain of the postsynaptic density protein PSD-95 in neurons. *J. Neurosci.* **24,** 865–876
35. Lai, K. O., and Ip, N. Y. (2009) Recent advances in understanding the roles of Cdk5 in synaptic plasticity. *Biochim. Biophys. Acta* **1792,** 741–745
36. Schmetsdorf, S., Arnold, E., Holzer, M., Arendt, T., and Gärtner, U. (2009) A putative role for cell cycle-related proteins in microtubule-based neuroplasticity. *Eur. J. Neurosci.* **29,** 1096–1107